Analysis of experimental unsteady wall pressure data from a jet installed above a semi-finite plate

Stefano Meloni, Jack L. T. Lawrence, Anderson R. Proença, Alessandro Trotta, Roberto Camussi, Rod H. Self

ANALYSIS OF EXPERIMENTAL UNSTEADY WALL PRESSURE DATA FROM A JET INSTALLED ABOVE A SEMI-FINITE PLATE

Stefano Meloni[1] **Jack L.T. Lawrence**[2] **Anderson R. Proença**[2]
Alessandro Trotta[1] **Roberto Camussi**[1] **Rod H. Self**[2]
[1] Department of Engineering, University of RomaTre, Rome, 00146, RM, Italy
[2] Institute of Sound and Vibration Research, University of Southampton, Southampton, SO17 1BJ, Hampshire,UK
stefano.meloni@uniroma3.it,

ABSTRACT

An investigation into the installation noise from a semi-finite flat plate next to a jet was performed. The experiment was carried out in the ISVR's anechoic Doak Laboratory, at the University of Southampton, using wall pressure transducers flush mounted on the plate surface and a far-field microphone array. In order to reproduce a setup representative of a real scaled jet-wing configuration the plate trailing edge was located at three nozzle exit diameters axially downstream of the jet exhaust. The radial position of the plate was varied from 0.76 to 1.50 nozzle exit diameters from the jet axis to the plate surface. The jet Mach number was also varied from 0.3 up to 0.9. The wall pressure transducers were positioned in the streamwise direction parallel to the jet center-line on the plate surface, including one position upstream of the nozzle exhaust. Data analyses were performed using multivariate statistical quantities in the time and frequency domains. Wall pressure data were correlated with the far field signals illustrating the propagation effects of the detected wall pressure signatures.

1. INTRODUCTION

In the last 50 years the number of people that are demanding to fly is increased, this induced a growing of the airports and aircraft size. This provides a significant increase of the environmental noise pollution around airports. In order to enhance these noise emissions stringent regulations are released by the international civil aviation, moving manufactures to reduce the noise emissions.

One of the main noise sources in the commercial aircraft is jet noise. This source was massively studied in the last century determining an high dependence of the noise emitted by jets on the nozzle exhaust velocity [1–3]. These results, together to the necessity to improve the aero and thermodynamic efficiencies of modern turbofans, moved the engines industries to increase the nozzle by pass ratio producing now Ultra-High-Bypass-Ratio engines, hence maintaining the same level of thrust and reducing the jet exhaust velocity. Nevertheless, the introduced configuration has an higher nozzle exhaust diameter and in order to respect the ground clearance this engines configuration leads to a closer coupled jet-wing layout. That said, nowadays the interactions effects, called installation effects are an important research topic.

Several studies were performed in the last years on the installed jet configuration, most of these mocking up the wing with a tangential flat plate and analyzing the modification of the far-field noise (see e.g. [4–6]).

A series of investigation on the modification of the jet velocity field due to the vicinity of a flat plate were reported in the literature, highlighting the presence of a soft Coandă effect [7, 8].

The interaction between the jet and a infinite flat plate was investigated in terms of wall pressure fluctuations, useful to understand the fluctuating wall pressure load over the wing and the vibro-acoustic response of the aircraft structural surfaces (see e.g. [9–13]). In the last few years some studies were performed on a real small scale jet-wing configuration [14–17], repeating the analysis also with an induced flight stream, provided by a wind tunnel.

The task of this work is an investigation of the installation effects in terms of both wall pressure fluctuations and far-field noise. The analysis was performed at different jet Mach numbers from $M_j = 0.5$ to $M_j = 0.9$ thus investigating the high subsonic regime. The position of the the semi-finite flat plate was varied from $H/D = 0.76$ to $H/D = 1.5$, thus considering different jet plate interaction levels.

Wall pressure fluctuations were investigated using flush mounted wall pressure transducers installed on the projection of the jet center-line over the wing pressure side, fixing also one axial position before of the nozzle exhaust. Far field measurements were performed using a polar array of $B\&K$ microphones. Data analysis was performed in terms of multivariate statistics in both time and frequency domain, performing also a study of the coherence between wall pressure and far-field signals.

Details about the experimental setup are given in Sec.II and the results dealing with the pressure statistics are reported in Sec. III. Final conclusions are presented in Sec. IV.

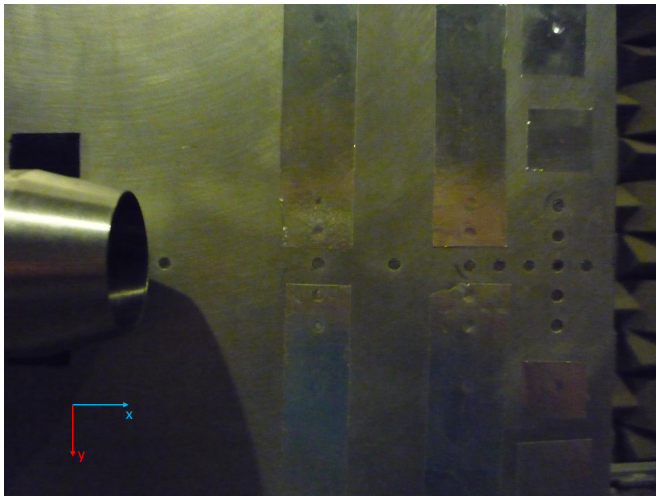

Figure 1. Experimental setup

2. EXPERIMENTAL SETUP

Experiments were carried out in the ISVR Doak Laboratory at the University of Southampton. The ISVR Doak Laboratory is an anechoic chamber, fully anechoic above 400 Hz. The facility has dimensions approximately of 15 m-long, 7 m-wide and 5 m-high. Details are reported in [4]. A single stream unheated jet with a diameter (D) of $38.1mm$ is installed in the anechoic chamber and connected to high-pressure compressor reservoir system, with a maximum pressure of 20 bar. The jet spreading half angle, evaluated via hot-wire measurements of the jet velocity field, is around 7°, as reported in previous works [18, 19].

In order to simulate a wing surface, an horizontal semi-finite flat plate was installed close to the jet flow and aligned using a 2-axis traverse system. The total length of the plate was $20D$, while the span lengthy was around $25D$, hence being sufficiently large to prevent the additional noise from the flow passing over the side edges. The plate was termed semi-finite and the plate trailing edge was machined down (at an angle of 60°) to a thickness of $1mm$. The initial thickness was $1cm$. A series of holes were manufactured over the plate surface to insert wall pressure transducers. Measures were performed fixing the position of the plate trailing edge at $L/D = 3$ from the nozzle exhaust, thus simulating a configuration close to a real scaled jet-wing architecture. A picture of the experimental setup is reported in Figure 1. The frame of reference is fixed at the nozzle exhaust on the jet center-line and oriented as reported into the Figure 1

The jet Mach number was varied from $M_j = 0.5$ to $M_j = 0.9$, thus carrying out a complete investigation from the slightly-compressible regime to the highest subsonic flow region. The radial position of the flat-plate was also varied from $H/D = 0.76$ to $H/D = 1.5$ investigating different jet-plate interaction levels.

Measures were performed in terms of wall pressure fluctuations and far-field signals. The wall pressure fluctuations were acquired using flush mounted wall pressure

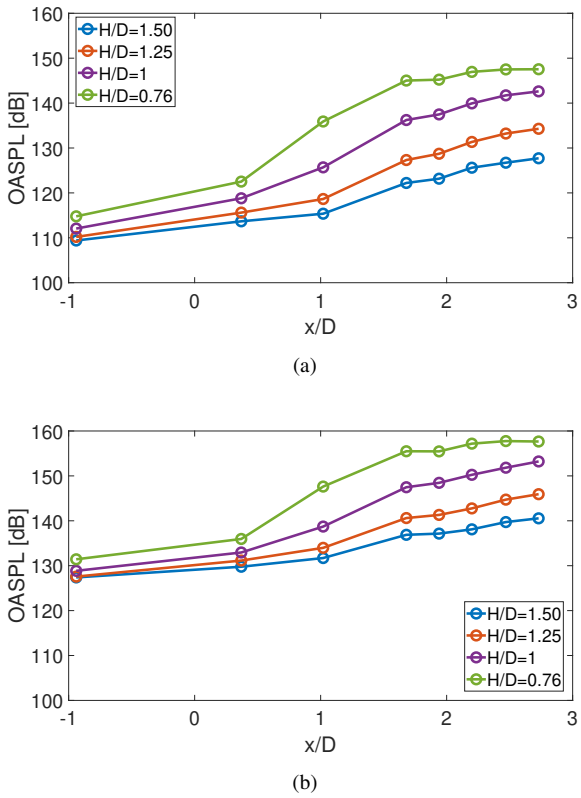

Figure 2. Axial evolution of the wall pressure OASPL for different radial positions of the flat plate: (a) At $M_j = 0.5$. (b) At $M_j = 0.9$

transducers (Kulite Type XT-190) with a sensing diameter of $2mm$. Signals were acquired at a sampling frequency of $50kHz$ and for a time of $9s$. Far-field signals were acquired using an array of $B\&K$ microphones for an acquisition time of $9s$. The sampling frequency was set like for the wall pressure fluctuations at $50kHz$.

3. RESULTS

3.1 Wall pressure field

The first part of the results is presented in terms of Overall Sound Pressure Level (OASPL) evaluated as follows:

$$OASPL = 10\log_{10}\left(\frac{\sigma_p^2}{P_{ref}^2}\right), \tag{1}$$

where σ_p is the standard deviation of the pressure signal (p) and P_{ref} is the reference pressure that measures $20\mu Pa$.

According to [11] the trend of the OASPL is not affected by different jet Mach numbers, as shown in Figure 2 (a)(b). Moreover, moving the flat plate closer to the jet flow an important increase of the OASPL is detected, specially at higher x/D. Nevertheless, considering the pressure transducers positioned at $x/D = -0.94$, signals are soft affected by the different plate positions, for both jet Mach numbers. The over all statistical analysis is deepened using kurtosis evaluated as follows:

$$k = \frac{E(p-\mu)^4}{\sigma_p^4}, \tag{2}$$

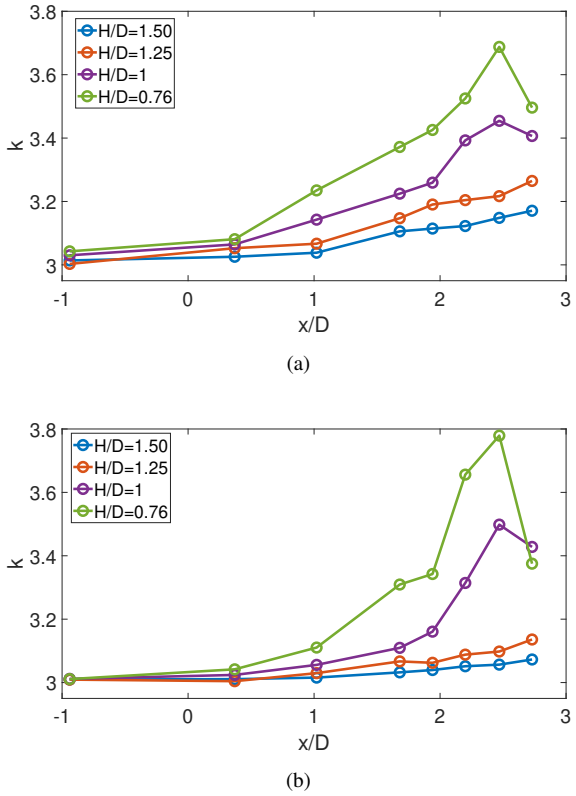

Figure 3. Axial evolution of the wall pressure kurtosis for different radial positions of the flat plate: (a) At $M_j = 0.5$. (b) At $M_j = 0.9$

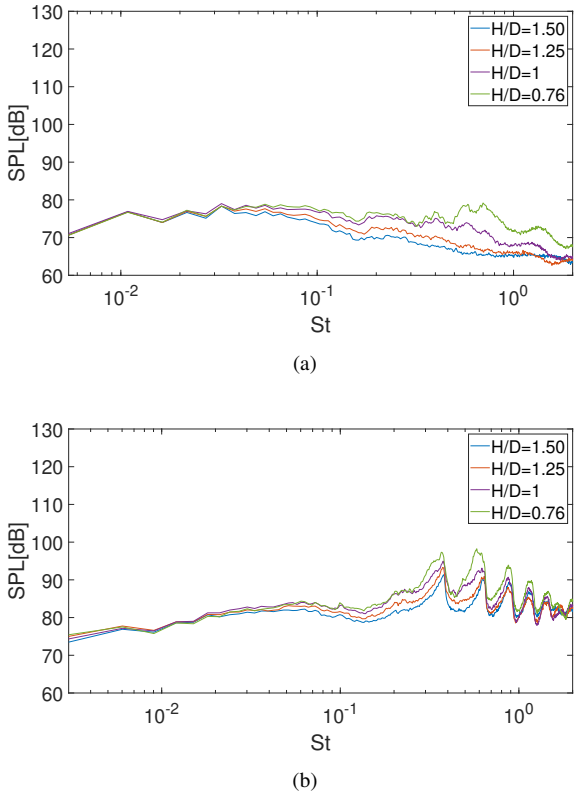

Figure 4. Pressure autospectra at $x/D = -0.94$ for different radial positions of the flat plate: (a) At $M_j = 0.5$. (b) At $M_j = 0.9$

where μ is the mean of the signal p and E() is the expected value. Wall pressure kurtosis trends are reported in the Figure 3.

Kurtosis close to 3 is detected when the radial position of the flat plate is positioned at $H/D = 1.5$, whit a slight increase going close to the trailing edge. This means that in this configuration the wall pressure field over the flat plate is few influenced by the jet hydrodynamic field. Moreover, a softly higher kurtosis is detected at the lower jet Mach number, Figure 3(a) at H/D=1.5.

On the other hand, a different trend is detected at $H/D = 0.76$ and $H/D = 1$, where the kurtosis starts to increase from the firsts axial locations downstream of the nozzle exhaust. In this two configurations a kurtosis peak is highlighted, in the transducer positioned before than the trailing edge, with a subsequent rapid decay. This effect is not present using an infinite plate [9, 11] it is probably due to the interaction between the jet flow and the plate trailing edge. Comparing Figure 3(a) and 3(b) the kurtosis trend, is slightly affected by different jet Mach numbers.

For all the plate locations and all the jet flow conditions a kurtosis close to three is detected using the signal provided by the pressure transducers positioned upstream of the nozzle exhaust.

The single point statistics were evaluated in the frequency domain using the Sound Pressure Level (SPL), as following reported:

$$SPL = 10 \log_{10}\left(\frac{PSD\Delta f_{ref}}{P_{ref}^2}\right), \tag{3}$$

PSD is the power spectral density evaluated using the Welch method, $\Delta f_{ref} = 1Hz$ is the bandwidth. SPLs are plotted using the Strouhal number evaluated as follows:

$$St = \frac{fD}{U_j}, \tag{4}$$

where D is the nozzle exhaust diameter and U_j the nozzle exhaust velocity.

In the Figure 4 are reported the pressure autospectra at $x/D = -0.94$, thus in a upstream position, respect to the nozzle exhaust, not influenced by the jet hydrodynamic field. A series of peaks are detected at all the radial positions of the flat plate only at $M_j = 0.9$, Figure 4(b). These are probably related to upstream jet travelling modes as discussed by Jordan et al. [20] for near field measurements. According to [14], which investigates the presence of these modes using the wall pressure fluctuations in real scaled wing configurations, the frequency range of these peaks varies from $St = 0.5$ to $St = 1$. Peaks look not influenced by the radial position of the flat plate except at $H/D = 0.76$, where an higher energy content is detected. On the other hand, according to [20] peaks are not detected at $M_j = 0.5$, although a broadband energy

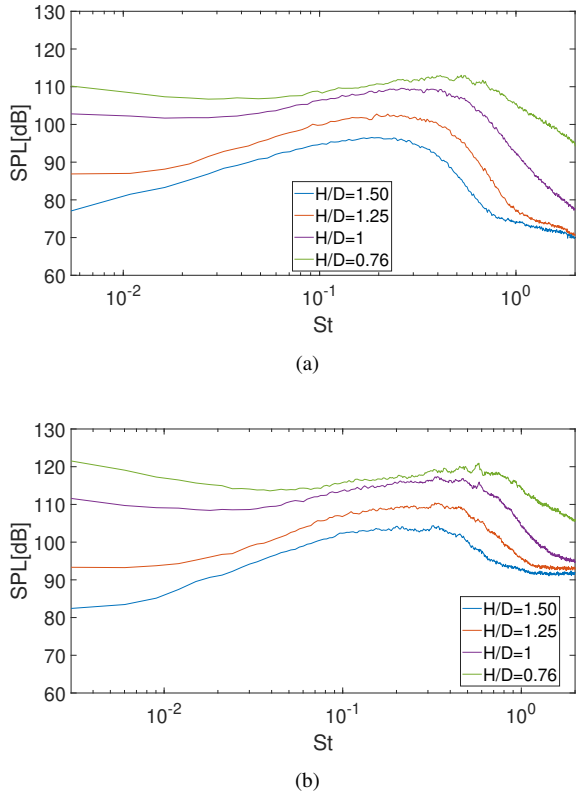

Figure 5. Pressure autospectra at $x/D = -2.73$ for different radial positions of the flat plate: (a) At $M_j = 0.5$. (b) At $M_j = 0.9$

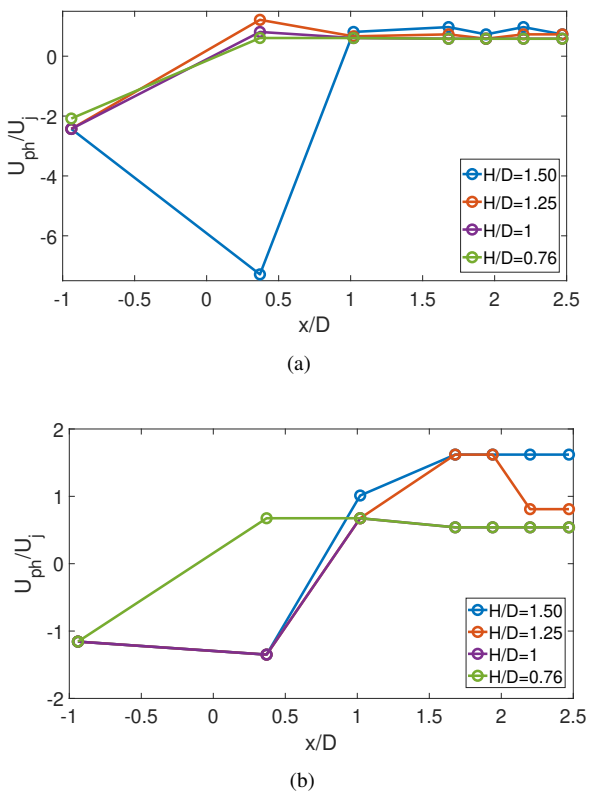

Figure 6. Axial evolution of the wall pressure phase speed for different radial positions of the flat plate: (a) At $M_j = 0.5$. (b) At $M_j = 0.9$

content increase is highlighted reducing the distance between the plate and the jet axis, as pointed out in Figure 4(a). Taking into account again Figure 4(a) soft peaks are detected at $H/D = 0.76$, this effect is probably related to the presence of a series of less energetic upstream modes generated by the interaction between the jet flow and the plate trailing edge. To carry out a complete physical explanations further investigations are necessary.

The autospectra were also reported in Figure 5 considering the pressure transducer closer to the wing trailing edge.

Spectra shape are slightly influenced by the jet Mach number. As reported in the Figure 5 (b) the increase of the jet Mach number reduces the hydrodynamic bump at the range of the St comprises between $St = 0.1$ and $St = 0.8$. At both jet Mach numbers the shape of the spectra reported in the Figure 5 are very influenced by the various positions of the flat plate, this is ascribed to different interactions between the plate surface and the jet exhausted flow structures.

Two point statistics were used to evaluated the wall pressure phase speed, as reported in the following equation:

$$U_{ph} = \frac{\xi}{\tau}, \tag{5}$$

where ξ is the distance between two consecutive pressure transducers and τ is the cross-correlation first peak time delay.

The phase speed trends are reported in the Figure 6 for different jet Mach numbers and different positions of the flat plate.

The wall pressure phase speed looks not influenced by different locations of the flat plate at $M_j = 0.5$, Figure 6 (a). Different results are detected at $M_j = 0.9$, indeed considering only the Kulite locations downstream of the nozzle exhaust, the phase speed at $H/D = 0.76$ and $H/D = 1$ is the same with a value close to 0.6 of the jet velocity and a slight decrease going more downstream. Whereas an higher phase speed close to the sound speed velocity is detected at $H/D = 1.25$ and $H/D = 1$. This is ascribed to the different interaction between the flow and the flat plate. As it is possible to see in the Figure 6 (b), the phase speed at $H/D = 1.25$ decreases at the trailing edge taking a trend similar to the lower H/D.

Whereas, considering the upstream microphone, a phase speed close the sound speed is detected in all cases. Observing, Figure 6 (b) a different trend at $H/D = 0.76$ is detected close to the nozzle exhaust, probably due to the vicinity of the plate that induces some hydrodynamic effects over the pressure transducers.

3.2 Far-field

The far-field is investigated in terms of single point statistics using the OASPL evaluated in the equation (1). In Figure 7 are reported the OASPL trends for different jet Mach numbers and different H/D positions.

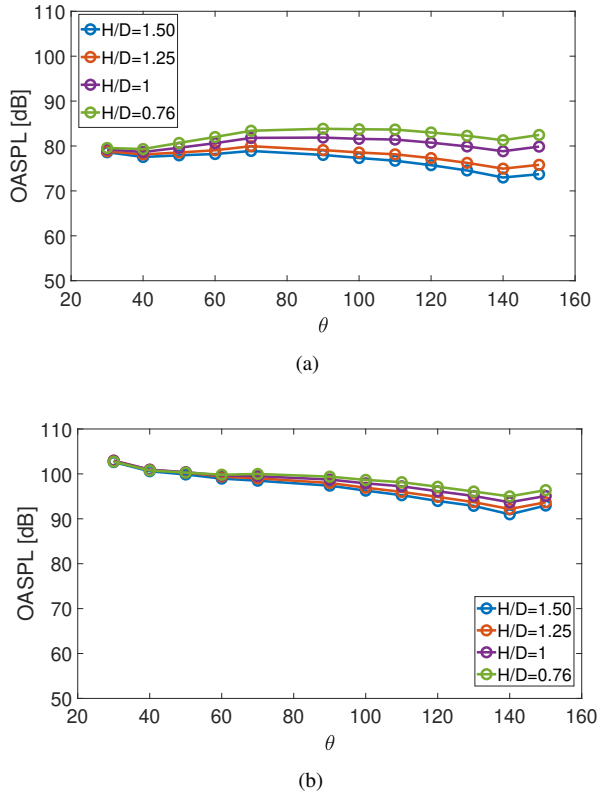

Figure 7. Evolution of the far-field OASPL for radial positions of the flat plate: (a) At $M_j = 0.5$. (b) At $M_j = 0.9$

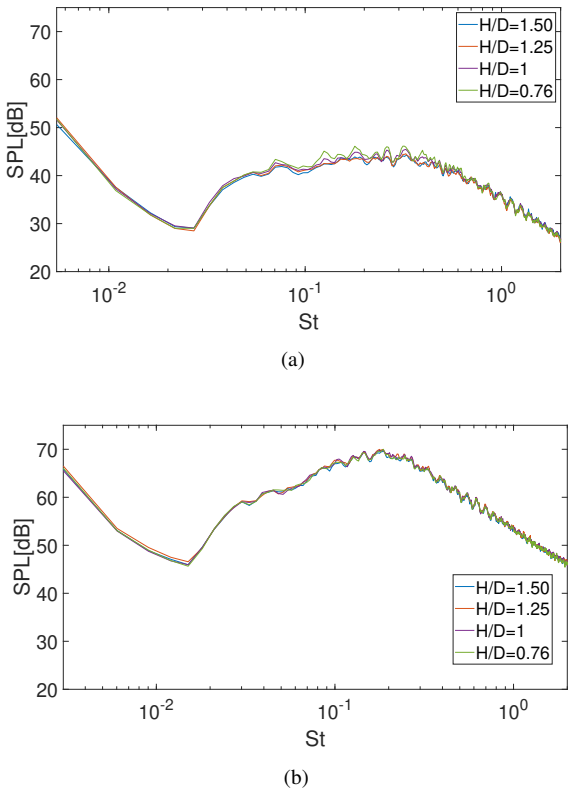

Figure 8. Far-field autospectra at $\theta = 30°$ for different radial positions of the flat plate: (a) At $M_j = 0.5$. (b) At $M_j = 0.9$

The OASPL in far-field is influenced by the different radial positions of the flat plate, specially at the lower Mach numbers Figure 7(a). As it is possible to see, this effect is more evident at the higher polar angles which are related to microphones positioned upstream of the nozzle exhaust. Whereas, considering lower polar angles, the different radial plate positions induce less evident effects. Observing In Figure 7(b) it is clear that the plate's influence decreases with increasing the jet Mach number.

The far-field analysis, has been deepened evaluating the pressure autospectra, reported in term of SPL as defined in the equation (3). In Figure 8 are reported the pressure autospectra at $\theta = 30°$

A not detectable effect is carried out varying the position of the flat plate at both jet Mach numbers and for all the frequencies range.

Furthermore, pressure autospectra at $\theta = 150°$ are reported in the Figure 9. At this polar location the spectra energy content is increased reducing the radial distance of the flat plate from the jet axis, especially at $M_j = 0.5$, Figure 9 (a). This effect is located at the highest frequencies. While at $M_j = 0.9$, this spectra increasing is reduced and localized in a series of peaks, Figure 9(b). Moreover an energy peak localized $St = 0.5$ appears at $H/D = 1$ and it is increased reducing the radial position of the flat plate.

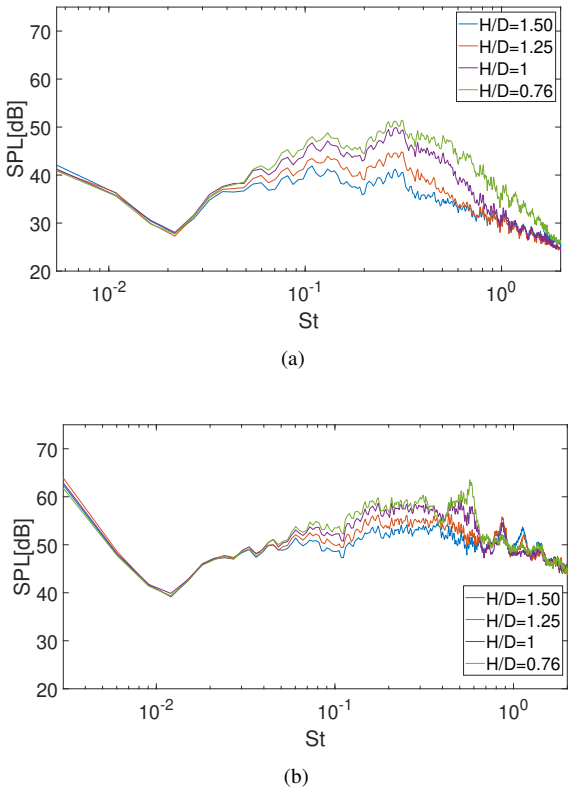

Figure 9. Far-field autospectra at $\theta = 150°$ for different radial positions of the flat plate: (a) At $M_j = 0.5$. (b) At $M_j = 0.9$

3.3 Wall pressure/Far-field coherence

In order to deepen the differences in terms of noise detected at $\theta = 150°$, the coherence between wall pressure fluctuations and far field noise is reported in this section. According to [11] the coherence function was evaluated as follows:

$$\gamma(\xi,\omega) = \frac{|CPSD_{p_1p_2}(\xi,\omega)|}{[PSD_{p_1}(\omega)PSD_{p_2}(\omega)]^{\frac{1}{2}}}, \qquad (6)$$

where ω is the angular frequency, $CPSD_{p_{far}p_{wp}}$ is the cross-spectrum between wall pressure and far-field signals, while $PSD_{p_{far}}$ and $PSD_{p_{wp}}$ are respective auto-spectra of the signals considered, ξ is the separation distance. The far-field microphone is fixed using the microphone positioned at $\theta = 150°$

Figure 10 shows the wall pressure/far-field coherence at $M_j = 0.5$ for different radial positions of the flat plate. An high coherence is detected at $H/D = 0.76$ between the far-field signal at $\theta = 150°$ and the signals acquired by wall pressure transducers positioned upstream of the nozzle exhaust, Figure 10(a). While at the trailing edged an important coherence is detected only for a short frequency range, probably cause of a strong presence of turbulent boundary effects that not propagate toward the far-field. As it is possible to see in Figure 10, moving the radial position of the flat plate to $H/D = 1.5$ the coherence between far-field and wall pressure at the trailing edge increase. This is probably due to the reduction of the jet plate interaction that erases the contribute of boundary layer on the wall pressure spectra; confirming the assertion that boundary layer effects are not correlated to the far-field noise. On the other hand, considering the pressure transducers located at a lower axial position the coherence between far-field and wall pressure signal decrease within the increase of the radial distance between the jet flow and the plate surface probably due to the reduction of the jet trailing edge interaction.

The analysis is repeated at $M_j = 0.9$ and reported in the Figure 11.

The increase of the jet Mach number reduces the magnitude of the wall pressure/far-field coherence for all the radial positions of the plate. Although, the effects is terms of coherence shape are generally not varied if compared with the same at $M_j = 0.5$

4. CONCLUSIONS

An investigation in terms of wall pressure fluctuations and far-field noise was performed mocking up the wing with a semi-finite flat plate. Experiments were performed into a semi-anechoic chamber varying both the radial position of the flat plate and the jet Mach numbers. Different interaction levels were detected in terms of wall pressure OASPL for various plate locations, and various jet Mach numbers. This difference is also observed in terms of kurtosis highlighting strong interactions between the jet flow and the trailing edge only at lower H/D. The plate effects on the jet pressure fields were deepened in the frequency domain using the SPL. Considering the pressure transducer located

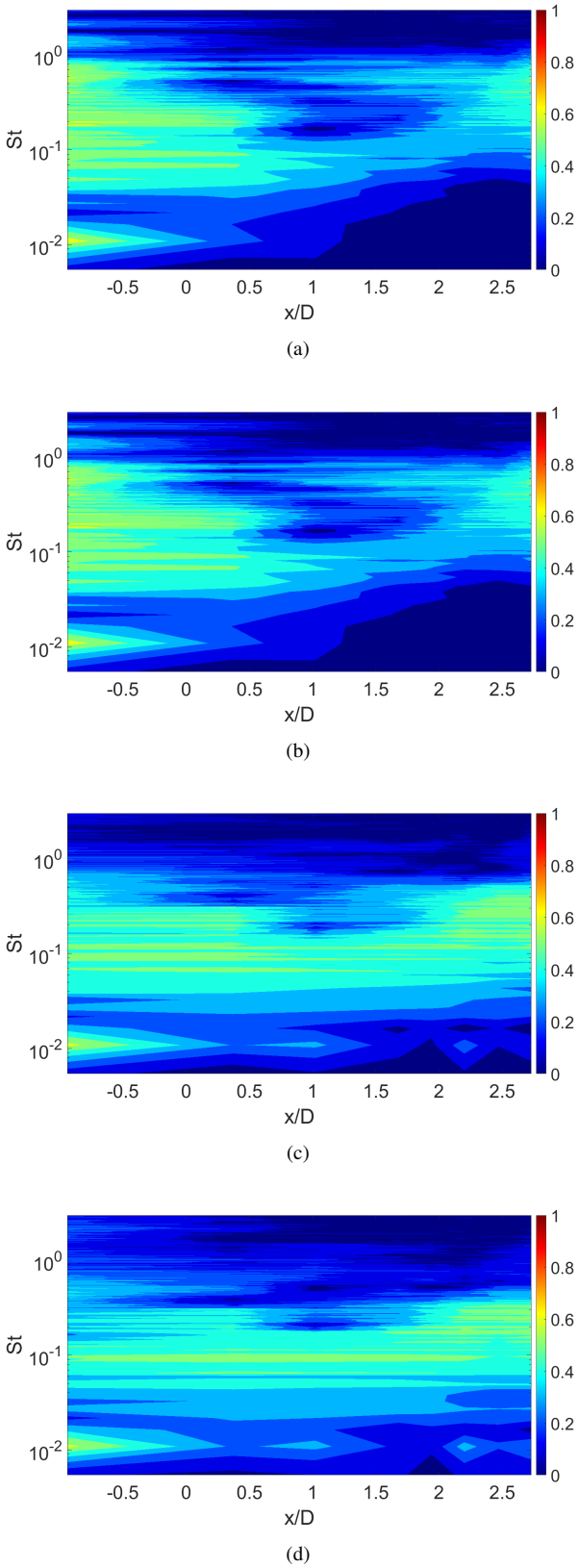

Figure 10. Wall pressure/Far-field coherence at $\theta = 150°$ for different radial positions of the flat plate at $M_j = 0.5$. (a) $H/D = 0.76$; (b) $H/D = 1$; (c) $H/D = 1.25$; (d) $H/D = 1.5$;

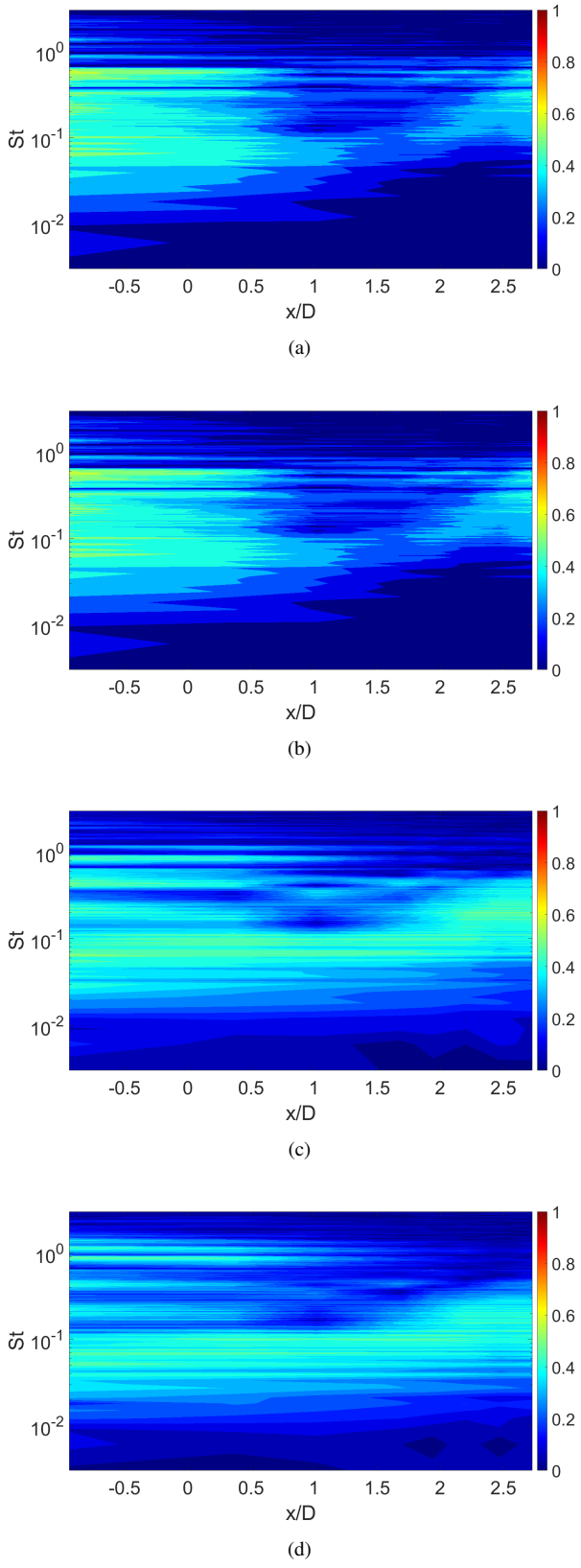

Figure 11. Wall pressure/Far-field coherence at $\theta = 150°$ for different radial positions of the flat plate at $M_j = 0.9$. (a) $H/D = 0.76$; (b) $H/D = 1$; (c) $H/D = 1.25$; (d) $H/D = 1.5$;

upstream of the nozzle exhaust an important influence of plate position is highlighted at $M_j = 0.5$ in the higher frequencies. This effect is reduced at $M_j = 0.9$. Nevertheless, a series of peaks slightly influenced by the radial position of the flat plate are detected at $M_j = 0.9$. Two point statistics were also evaluated investigating the effect of the different plate positions on the wall pressure phase speed. Results showed that the wall pressure phase speed trend is very influenced by the plate location at $M_j = 0.9$, while at $M_j = 0.5$ a not visible effect is detected.

Moreover the analysis has been completed by the far-field investigation, highlighting an important influence of the different plate locations at higher polar angles and at the lowest jet Mach number.

Finally, wall pressure/far-field coherence is reported, considering the microphone at $\theta = 150°$, thus in the position where the maximum installation effect is detected in far-field analysis, and all the wall pressure transducers. It is highlighted that the mechanisms which influence the far-field noise are mostly related to both: the wall pressure transducers positioned upstream of the nozzle exhaust and at the wing trailing edge. A strong influence is detected varying the jet Mach number and the radial positions of the flat plate.

5. REFERENCES

[1] M. J. Lighthill, "On sound generated aerodynamically," *General theory. Proc. R. Soc. Lond.*, pp. 564–587, 1952.

[2] G. Lilley, "On the noise from air jets.," *AGARD CP 131*, pp. 13.1–13.2, 1974.

[3] J. E. F. Williams and L. H. Hall, "Aerodynamic sound generation by turbulent flow in the vicinity of a scattering half plane," *Journal of Fluid Mechanics*, vol. 40, no. 4, p. 657–670, 1970.

[4] J. Lawrence, M. Azarpeyvand, and R. Self, "Interaction between a flat plate and a circular subsonic jet," in *17th AIAA/CEAS Aeroacoustics Conference (32nd AIAA Aeroacoustics Conference)*, 2011.

[5] B. Lyu, A. P. Dowling, and I. Naqavi, "Prediction of installed jet noise," *Journal of Fluid Mechanics*, vol. 811, p. 234–268, 2017.

[6] A. V. Cavalieri, P. Jordan, W. R. Wolf, and Y. Gervais, "Scattering of wavepackets by a flat plate in the vicinity of a turbulent jet," *Journal of Sound and Vibration*, vol. 333, no. 24, pp. 6516 – 6531, 2014.

[7] A. Proença, J. Lawrence, and R. Self, "Investigation into the turbulence statistics of installed jets using hot-wire anemometry," *Experiments in Fluids*, vol. 61, no. 220, p. 19, 2020.

[8] S. Meloni, A. Di Marco, E. de Paola, R. Camussi, and G. Fava, "Pressure and velocity measurements of a compressible jet interacting with a flat plate," in

Progress in Turbulence VIII, pp. 271–276, Springer International Publishing, 2019.

[9] A. Di Marco, M. Mancinelli, and R. Camussi, "Pressure and velocity measurements of an incompressible moderate reynolds number jet interacting with a tangential flat plate," *Journal of Fluid Mechanics*, vol. 770, p. 247–272, 2015.

[10] S. Meloni, R. Camussi, A. Di Marco, and M. Mancinelli, "Single and multivariate statistics of jet-induced pressure fluctuations over an infinite plate," *Applied Sciences*, vol. 10, no. 13, 2020.

[11] S. Meloni, A. Di Marco, M. Mancinelli, and R. Camussi, "Wall-pressure fluctuations induced by a compressible jet flow over a flat plate at different mach numbers," *Experiments in Fluids*, vol. 60, p. 48, Feb 2019.

[12] S. Meloni, R. Camussi, A. D. Marco, and M. Mancinelli, "Experimental investigation of jet-induced wall pressure fluctuations over a tangential flat plate at two reynolds numbers," *Sci. Rep*, 2020.

[13] S. Meloni, J. L. Lawrence, A. R. Proença, R. H. Self, and R. Camussi, "Wall pressure fluctuations induced by a single stream jet over a semi-finite plate," *International Journal of Aeroacoustics*, vol. 0, no. 0, p. 1475472X20930650, 2020.

[14] S. Meloni, M. Mancinelli, R. Camussi, and J. Huber, "Wall-pressure fluctuations induced by a compressible jet in installed configuration," *AIAA Journal*, vol. 58, no. 7, pp. 2991–3000, 2020.

[15] J. Lawrence, "Aeroacoustic interactions of installed subsonic round jets," July 2014.

[16] V. Mengle, "The effect of nozzle-to-wing gulley height on jet flow attachment to the wing and jet-flap interaction noise," in *17th AIAA/CEAS Aeroacoustics Conference (32nd AIAA Aeroacoustics Conference)*, 2012.

[17] J. Huber, P. Jordan, M. Roger, Y. Gervais, D. Lizarazu, and F. Wlassow, "Exploring flight effects for installed jet noise using wavepacket sound-source model," *AIAA paper 2017-3382. 23nd AIAA/CEAS Aeroacoustics Conference Denver, Colorado, USA*, 2017.

[18] A. Proença, *Aeroacoustics of isolated and installed jets under static and in-flight conditions*. PhD thesis, University of Southampton, March 2018.

[19] A. Proença, J. Lawrence, and R. Self, "Measurements of the single-point and joint turbulence statistics of high subsonic jets using hot-wire anemometry," *Experiments in Fluids*, vol. 60, no. 4, p. 63, 2019.

[20] P. Jordan, V. Jaunet, A. Towne, A. V. G. Cavalieri, T. Colonius, O. Schmidt, and A. Agarwal, "Jet–flap interaction tones," *Journal of Fluid Mechanics*, vol. 853, p. 333–358, 2018.